Published article:

T. R. B. Kushal and M. S. Illindala, "Decision Support Framework for Resilience-Oriented Cost-Effective Distributed Generation Expansion in Power Systems," *IEEE Trans. Ind. Appl.*, vol. 57, no. 2, pp. 1246–1254, 2021, doi: 10.1109/TIA.2020.3047595.

Decision Support Framework for Resilience-Oriented Cost-Effective Distributed Generation Expansion in Power Systems

Tazim Ridwan Billah Kushal
Student Member, IEEE
The Ohio State University
2015 Neil Ave, Dreese Lab 205
Columbus, OH 43210, USA
kushal.1@osu.edu

Mahesh S. Illindala
Senior Member, IEEE
The Ohio State University
2015 Neil Ave, Dreese Lab 205
Columbus, OH 43210, USA
millindala@ieee.org

***Abstract*—Resilience of electricity grids to rare but severely disruptive events, such as natural disasters, has emerged in recent years as an important aspect in power system planning. Development of resilience-oriented techniques are needed due to the limitations of reliability-oriented methods in addressing large unexpected outages. This paper presents a novel decision analysis approach to enhance the resilience of a power distribution system by leveraging the distributed nature of solar photovoltaic (PV) and battery energy storage system (BESS) resources. The proposed decision-making framework uses analytic hierarchy process (AHP) to evaluate different possible allocations of PV and BESS resources to load buses for multiple contingencies based on resilience enhancement and cost. Each allocation plan provides the size of PV arrays and BESS units to be installed at each bus within the distribution system. A deterministic formulation ranks line outage scenarios based on unserved load. The trade-off between cost and resilience is modeled via cost-effectiveness analysis (CEA) that indicates the preferability of each allocation plan. The main contribution of this paper is the development of an adaptable and computationally feasible decision support framework to determine cost-effective configurations of PV arrays and BESSs for mitigating the effects of power line outage contingencies. To evaluate the proposed framework, a case study is carried out on the IEEE 33-bus radial distribution system. The results show that the proposed method can offer effective guidance to the planner for making informed investment decisions and achieving cost-effective resilience enhancement.**

***Index Terms*—Decision support systems, distributed generation, power system planning, resilience, renewable energy**

I. Introduction

Traditional electric power systems are designed to operate during certain contingencies based on the reliability criteria of security and adequacy. In reliability-oriented planning, expected failures with predictable impacts are modeled stochastically using metrics such as System Average Interruption Duration Index (SAIDI) and System Average Interruption Frequency Index (SAIFI), although the exact moment of occurrence is not known in advance [1]. When planning for failure scenarios, more probable $N-1$ contingencies are prioritized over more numerous but less probable $N-k$ contingencies [2]. However, catastrophic events such as natural disasters or deliberate attacks, which occur rarely but have a large and unpredictable impact, present a challenge to this reliability-based planning of power systems. According to data from the North American Electric Reliability Council (NERC), 933 blackouts were reported between 1984 and 2006, each affecting tens or even hundreds of thousands of customers [3]. Weather-related events can cause massive disruption of the grid in the form of infrastructure damage and service interruption. In the period 2003-2012, over 50,000 U.S. customers were impacted by 679 power outages due to weather-related events [4]. Hurricane Harvey was estimated to have caused $125 billion in total damages and power outage to about 220,000 customers [5]. Several Caribbean islands and the U.S. state of Florida suffered extensive damage from Hurricane Irma, which caused widespread destruction of power lines and almost total loss of electricity in Puerto Rico [6]. Aside from physical events, modern industrial control systems such as the power grid also present cybersecurity challenges due to the possibility of malicious cyber attacks [7]. The modernization of the grid and its transformation into a cyber-physical system means that physical disruption can also be caused by cyber attacks, such as those injecting false data into communications to impact operation [8]–[10]. Significance of cyber threats to power grid operation is demonstrated by the recent BlackEnergy and Triton/TRISIS malware attacks against targets in Ukraine and the Middle East respectively [11]. The BlackEnergy attack has been studied in detail and found to have caused about 225,000 customers to lose power [12]. Addressing such high-impact and unpredictable contingencies through methods traditionally used in reliability-oriented planning faces two major limitations. Firstly, the rarity of such events introduces problems with stochastic modeling due to the possibility of incorrectly estimating risk exposure, a phenomenon known as *ludic fallacy* [13]. Unlike lower-order contingencies, forecast errors can be unacceptably large since, for a given accuracy, the magnitude of error will be higher for high-impact events. Secondly, even if forecast errors are accounted for through redundant capacity (by adding more lines and/or generators),

there is the issue of large investment in resources that will be under-utilized most of the time, since severe disruptions are rare.

Resilience was defined in the Presidential Policy Directive 21 as the ability of a system to adapt to varying conditions, withstand disruptive events, and recover from them [14]. It is a concept distinct from reliability and indicates the ability of a system to mitigate the impact of low-frequency high-impact events, which cannot be captured by traditional reliability metrics such as SAIDI and SAIFI that often do not include large unexpected outages [15], [16]. A resilient system must maintain high levels of performance by anticipating, recovering from, and adapting to such disruptive events despite potentially unprecedented contingencies and severe, rapidly changing conditions [17]. In the context of power systems, this refers to the ability to minimize unserved electrical load during contingencies. Current practices with regard to distribution restoration leave the grid vulnerable to extreme weather events and are therefore not considered sufficiently resilient [18]. Probabilistic fragility modeling by Panteli et al. has shown that resilience-enhancing adaptation measures such as redundancy are necessary to ensure power system operation during extreme weather, particularly when key parameters such as wind speed are uncertain [19]. A study of the hazardous effects of wind storms in the Northeast U.S. using Sequential Monte Carlo simulations indicated the vulnerability of the grid to outage and the need for system hardening against wind storms [20]. Risk assessment modeling in [21] based on the application of data-mining techniques on historical outage data concluded that the U.S. electricity grid is especially vulnerable to severe wind events such as hurricanes and tornadoes that can affect overhead transmission and distribution systems. Although similar probabilistic methods have been used to ensure reliable power system operation [22] and planning [23], it is unclear how effective they are against rare extreme events, which are difficult to model stochastically due to their rarity. Therefore, additional resilience-oriented alternatives have been explored in the literature.

Researchers have proposed various methods of enhancing the resilience of power systems through planning, operational, and restorative measures [24]–[30]. One approach is to divide the grid into a number of smaller grids (islands) according to some grouping criteria to minimize load shedding and facilitate load restoration [24], [25]. A hierarchical outage management scheme has been used to design a resilient power distribution system encompassing multiple microgrids with distributed control [26]. Another method of quantifying resilience of a multi-microgrid system based on percolation theory was proposed in [27] and used to decide the priority of loads during service restoration. The feeder restoration approach presented in [28] uses distributed energy resources (DERs) to supply the critical loads in a power distribution system when the main grid supply is unavailable. Fang and Sansavini formulated resilience-oriented investment in transmission line expansion and switching devices as a tri-level optimization problem [29]. Optimal hardening of power distribution networks based on severity of weather events and vulnerability of lines is formulated as an optimization problem in [30]. Cost minimization, the common objective in these studies, is used to select optimal hardening strategies. It is trivial to show that higher resilience generally incurs higher costs. However, cost-effectiveness is useful for determining the return on investment for hardening strategies. Although optimal solutions are desirable, optimization-based formulations such as those presented in [29], [30] do not provide a simple, scalable computational framework for planners to evaluate the cost-effectiveness of strategies. Moreover, formulations such as [30] that consider worst-case scenarios may result in higher costs with little incremental benefits. On the practical side, running complex formulations such as tri-level optimization programs [29], [30] for large scenario sets is computationally expensive. In this paper, we propose an alternative methodology to analyze investment decisions based on cost-effectiveness, that ranks decisions (instead of providing an optimal one) and considers multiple contingencies of varying severity.

Recent research has focused on exploiting the potential of locally available generation by using DERs to improve the resilience of the electric grid, especially on the distribution side, which has been shown by past experience as the most vulnerable part of the infrastructure [31]. The authors of [31] mention solar photovoltaic (PV) devices as one the potential DERs. Several methods of optimally sizing PV systems have been proposed [32]–[36]. Additionally, PV arrays are coupled with energy storage such as battery energy storage system (BESS) to resolve the problem of intermittent power output [37] and control power injection rate for system stability [38], so that energy can be stored for use later instead of being curtailed as is the case of smart inverter active power injection control [39]. Their optimal sizing is generally treated as an optimization problem with a trade-off between cost and system reliability. Multi-objective approaches can include environmental considerations such as reduction of emissions (greenhouse gases and air pollutants) and fuel savings [34], [36]. Planning of renewable sources in power distribution networks brings additional challenges that requires meeting objectives regarding power quality, voltage stability, and profitability [40]–[42]. Such complex multi-objective optimization planning problems are made computationally tractable by metaheuristic algorithms, while analytical techniques are employed for modeling and validation [40].

The distributed nature of PVs can be useful in mitigating aggregation of large generation capacities at a limited number of nodes, which can be detrimental to resilience since many of the outages reported in [4] result from damaged transmission lines. A long-term planning study found that renewable power generators distributed throughout the system, in combination with small thermal units, can reduce dependence on bulk generation and transmission while maintaining reliability [43]. Also, previous works have modeled multiple outage scenarios using probabilistic methods. For example, Monte Carlo simulation is applied to model random outages in [23]. As

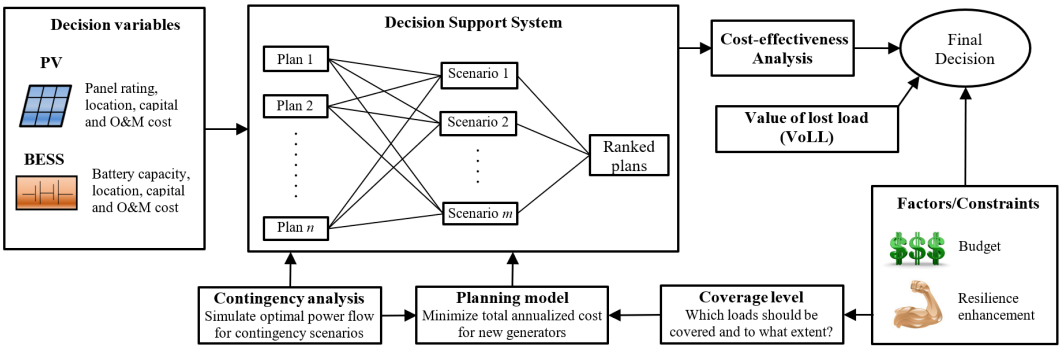

Fig. 1. Overview of the decision support framework.

discussed previously, this approach is unsuitable for resilience-oriented planning where the impact of outages is large and probability of occurrence is unknown.

This paper aims to enhance the resilience of a power grid by exploiting the distributed nature of PV systems, with BESS units added to resolve the intermittency issue. Redundancy-based adaptation measures such as this poses the problem of potentially allocating large amounts of resources for small gains, due to the uncertainty of extreme events, the impact of which cannot be modeled from historical data with sufficient accuracy, unlike load fluctuations and minor disruptions. The planner is faced with uncertainties regarding the amount of resources to allocate. Since adding more PV and BESS units would increase the resilience but would also cost more, cost-effectiveness analysis (CEA) is used to measure the performance (measured by the reduction in unserved load) per dollar spent. This paper enhances the systematic approach developed in [44], illustrated in Fig. 1, of ranking multiple allocation plans, evaluating alternatives and observing trends in cost-effectiveness for different levels of investment.

The proposed framework in Fig. 1 is organized into the following sections. Section II describes the methodology of contingency analysis, ranking allocation plans and the decision support tool. Section III explains the planning model, where PV and BESS resources are optimally allocated for each scenario. Case study of a radial power distribution system using the proposed framework is presented in Section IV. Section V concludes the paper.

II. Multi-contingency Planning

The ability of a power system to supply loads can be impaired in a variety of ways by extreme events. For example, power line outages, which prevent power flow through a subset of lines, can cause such disruptions. This can happen because of direct physical damage to the line or tripped circuit breakers due to overloading. Regardless of the reason, it often ultimately causes a supply shortfall that results in some unserved load. In this study, the amount of unserved load is used as the measure of system performance. Hence, resilience enhancement is defined as the reduction in total unserved load.

A. Contingency Analysis

The minimum unserved load under a given scenario may be determined by solving the cost-minimizing optimal power flow (OPF) problem, with a corresponding cost determined by the value of lost load (VoLL). Security-constrained OPF (SCOPF) can be used to deal with known contingencies by planning optimal corrective actions after a disruptive event [45]. However, the SCOPF formulation suffers from scaling problems. The order of contingency k, which in this study is the number of disabled branches in the distribution system, determines the number of scenarios. For a system with n branches, the number of possible contingencies with k lines disabled is $\binom{n}{k}$. The IEEE 33-bus test system has 32 branches (excluding the normally-open tie lines) and for k = 1, 2, 3 and 4 the number of scenarios is 32, 496, 4960 and 35960 respectively. Computational tractability decreases with the rapidly growing set of all possible scenarios. Robust programming approaches circumvent this problem by only selecting the worst contingencies using, for instance, a bi-level max-min formulation [46]. But this method has the disadvantage of increasing the cost by considering the worst possible scenario. This paper simulates the operating condition of the power system using conic programming, which offers a convenient way to solve OPF for radial AC systems using convex optimization [47]. The full non-convex optimization problem is reduced to a second-order cone programming (SOCP) problem by relaxing some equality constraints into inequality constraints and eliminating sinusoidal ones not required for radial load flow. The AC OPF is run for various contingencies and the unserved load results for each scenario are used in the decision process.

B. Analytic Hierarchy Process

The Analytic Hierarchy Process (AHP) is a numerical framework for complex multiple criteria decision making [48], allowing possible alternatives to be ranked based on numerically defined priorities instead of providing a single optimal solution. If the number of criteria considered in a decision process is m, then a $m \times m$ pairwise comparison matrix of criterion weights $\mathbf{A}$ can be defined so that the element a_{jk} expresses the importance of the j-th criterion relative to the k-th criterion. With n alternative options being

considered, a $n \times n$ pairwise comparison matrix $B^{(i)}$ can be constructed such that the element $b_{jk}^{(i)}$ indicates how preferable the j-th option is to the k-th option, with respect to the i-th criterion.

$$w_j = \frac{\sum_{k=1}^{m} \frac{a_{jk}}{\sum_{l=1}^{m} a_{lk}}}{m} \tag{1}$$

$$s_i^{(j)} = \frac{\sum_{k=1}^{n} \frac{b_{ik}^{(j)}}{\sum_{l=1}^{n} b_{lk}^{(j)}}}{n} \tag{2}$$

The pairwise comparison matrices are used to calculate the m-dimension criteria weight vector $\mathbf{w}$ and the n-dimensional option score vector $\mathbf{s}^{(j)}$ by normalization with the column sum and taking the row average, as shown in (1)–(2). The full $n \times m$ option score matrix is $\mathbf{S} = [\mathbf{s}^{(1)}\mathbf{s}^{(2)}...\mathbf{s}^{(m)}]$. As the final output, the AHP method assigns each option an overall score. The global score vector $\mathbf{v}$ gives the score for each option and is calculated as shown below.

$$\mathbf{v} = \mathbf{S}\mathbf{w} \tag{3}$$

All n options can be arranged from most desirable to least desirable by arranging them in descending order of scores. In this study, AHP has been used to solve the problem selecting the best allocation plan (size and location of PV and BESS units) for multiple scenarios, by considering the contingencies as criteria and the plans as options. Criteria weights are assigned based on the severity of the contingencies, as indicated by the unserved load. Option scores are decided based on the performance of the plans in each scenario, evaluated on the basis of the power supplied and the annual cost. Cost-effectiveness of one option relative to another is calculated using the CEA metric of incremental cost effectiveness ratio (ICER). Since a lower ICER means higher preferability, the utility score is defined as the inverse of ICER. After criteria weight and option score matrices are found, the final calculation of the global score vector has time complexity $\mathcal{O}(mn)$ for m contingencies and n options. Working memory requirements are also modest since the total number of matrix elements that need to be stored is m^2+mn+n. Therefore, the proposed AHP-based method can scale easily for much larger distribution systems than the test case.

$$u_i(j,k) = \frac{E_j^{(i)} - E_k^{(i)}}{C_j - C_k} \tag{4}$$

$$U_k = \sum_i \sum_j u_i(j,k) \tag{5}$$

$$CE_j^{(i)} = \frac{C_j}{E_j^{(i)} - E_o^{(i)}} \tag{6}$$

In (4), the utility of the j-th plan compared to the k-th plan for the i-th contingency is denoted by $u_i(j,k)$. $E_j^{(i)}$ and $E_k^{(i)}$ are the effects of the j-th and k-th plans, respectively, when they are applied to the i-th contingency, defined as the amount of load supplied. C_j and C_k are the annualized investment cost plus the annual operating cost of the j-th and k-th plans respectively. According to (4), a plan has higher utility if it supplies more power and has a lower annual cost, since a plan that can supply more power per additional dollar is considered to be more cost-effective. The total utility of the k-th plan U_k is calculated by summing over all the comparisons and contingencies as shown in (5). The average cost-effectiveness ratio for the j-th plan in the i-th contingency $CE_j^{(i)}$ is calculated as shown in (6), where $E_o^{(i)}$ is the active power supplied in that scenario without any additional generators.

$$x_{jk} = 1 + 8\left(\frac{\frac{1}{P_j^{US}} - \frac{1}{P_k^{US}}}{\max P^{US} - \min P^{US}}\right) \tag{7}$$

$$a_{jk} = \begin{cases} x_{jk} & : x_{jk} \geq 1 \\ \frac{1}{x_{jk}} & : x_{jk} < 1 \end{cases} \tag{8}$$

$$y_{jk}^{(i)} = 1 + 8\left(\frac{u_i(j,i) - u_i(k,i)}{u_{max}^{(i)} - u_{min}^{(i)}}\right) \tag{9}$$

$$b_{jk}^{(i)} = \begin{cases} y_{jk}^{(i)} & : y_{jk}^{(i)} \geq 1 \\ \frac{1}{y_{jk}^{(i)}} & : y_{jk}^{(i)} < 1 \end{cases} \tag{10}$$

Contingencies are compared on the basis of severity, which is represented by the amount of unserved load. P_j^{US} and P_k^{US} are the total unserved load in the k-th and j-th contingencies, respectively. Therefore, criteria are assigned importance by (7)–(8), where $\max P^{US}$ and $\min P^{US}$ are the maximum and minimum unserved load across all contingencies, respectively. Similarly, option scores are calculated in (9)–(10), with $u_{max}^{(i)}$ and $u_{max}^{(i)}$ denoting the maximum and minimum utility among all plans for contingency i, respectively, and $u_i(j,i)$ is the utility of plan j relative to no allocation plan in contingency i. Results of the contingency simulation are used as the basis for the planning model and decision support system, as shown in Fig. 1. It should be noted that the decision-maker is free to choose alternatives to the CEA-based utility formula presented here, as long as some minimal requirements are satisfied. An alternative method of calculating $u_i(j,k)$ should meet the basic requirement of quantifying preferability by assigning higher scores to better options and maintaining consistency. If option k_1 is better than k_2, then $u_i(k_1,k_2) > u_i(k_2,k_1)$. If both k_1 and k_2 are better than a third option k_3, then additionally $u_i(k_1,k_3) > u_i(k_3,k_1)$, $u_i(k_2,k_3) > u_i(k_3,k_2)$, and $u_i(k_1,k_3) > u_i(k_2,k_3)$.

III. Allocation and Sizing of PV and BESS

Power line outages reduce the number of available paths for power flow and may cause a shortfall in supply. Also, a disabled power line divides the grid into islands, which are groups of nodes with an existing path between each pair of nodes. Appropriately sized solar PV arrays, along with a BESS as a backup source and storage for excess energy, can supply the shortfall. In each island, the node with the highest unserved load across all the contingencies is selected for siting

TABLE I
PV PANEL PARAMETERS

PV panel	BP-Solar 3200
Rated power	200 W
Open-circuit voltage	30.8 V
Short-circuit current	8.7 A
Optimum voltage	24.5 V
Optimum current	8.16 A
Efficiency at STC	13%
Dimensions (L/W/D)	1680 × 837 × 50 mm
Cost per panel	$420
O&M cost	$15/kW

TABLE II
LEAD-ACID BATTERY PARAMETERS

Battery	Hoppecke 6OPzS 600
Rated capacity	600 Ah
Rated voltage	2 V
Minimum SOC	35%
Round-tip efficiency	85%
Max. charge/discharge rate	0.5 A/Ah, 0.5 A/Ah
Max. charge/discharge current	100 A/75 A
Self-discharge rate	1%
Dimensions (L/W/D)	215 × 193 × 710 mm
Cost per cell	$150
O&M cost	$20/kAh

these resources. Based on the results of AC OPF simulation described in Section II, the planning model allocates PV and BESS resources to each island to ensure that the demand is met at minimum cost.

$$\psi = 1 - \frac{P_d}{\sum_i P^{US}(i)}(1-c) \tag{11}$$

The fraction of the total load that is to be covered by the planning model is given by c. By default, it is assumed $c = 1$, although cases of $c < 1$ are also examined later in the case study. Sizing of the PV and BESS resources is based on the parameter ψ, which is calculated from c using the expression in (11), where P_d is the total load in the distribution system and $P^{US}(i)$ is the total load in island i for a particular contingency.

A. Photovoltaic Resources

A PV array equipped with a dc-ac inverter and a maximum power point tracking (MPPT) controller has a power output the depends on the solar irradiance and temperature. The PV array installed for island i is rated at $P^{(i)}_{pv\_r}$ with a derating factor of $f^{(i)}_{pv}$ to account for various factors such as shading and wiring losses. The actual power output of the array $P^{(i)}_{pv}$ depends on the on the solar insolation G and the temperature T. The solar radiation and temperature under standard test conditions are given by G_{STC} and T_{STC} respectively, while α_T is the temperature coefficient.

$$f(G;a,b) = \frac{\Gamma(a+b)}{\Gamma(a)\Gamma(b)}\left(\frac{G}{G_{max}}\right)^{a-1}\left(1-\frac{G}{G_{max}}\right)^{b-1} \tag{12}$$

$$P^{(i)}_{pv} = f^{(i)}_{pv} P^{(i)}_{pv\_r}\frac{G}{G_{STC}}[1+\alpha_T(T-T_{STC})] \tag{13}$$

$$P^{(i)}_{pv} \geq \frac{\psi}{\eta_{pv\_inv}} P^{US}(i) \tag{14}$$

The expression in (13) gives the instantaneous PV power output for a given solar radiation and temperature. Since solar irradiance changes with time, the output power also varies, so a stochastic model is needed to account for the time-varying nature and suggest an appropriate value for G. As in many previous studies, the insolation is assumed to follow a beta probability distribution function [49] given by (12), where a and b are the shape parameters of the beta distribution and Γ is the gamma function. Therefore, the allocated PV resources would have to be oversized in order to supply the demand. The PV rating $P^{(i)}_{pv\_r} = n^{(i)}_{pv} P_{pv\_unit}$ for island i is made up of $n^{(i)}_{pv}$ discrete units, each with rated power P_{pv_unit} . The minimum PV power output for each island i with unserved load $P^{US}(i)$ is given by (14), where η_{pv_inv} is the inverter efficiency. The full list of PV panel parameters is provided in Table I. Actual historical solar irradiance data has been used later in Section IV-B to account for solar and diurnal variations in insolation while evaluating the proposed scheme.

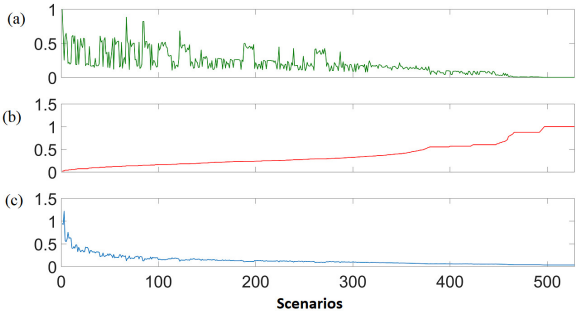

Fig. 2. Relationship between normalized (a) total unserved load, (b) cost, and (c) utility score.

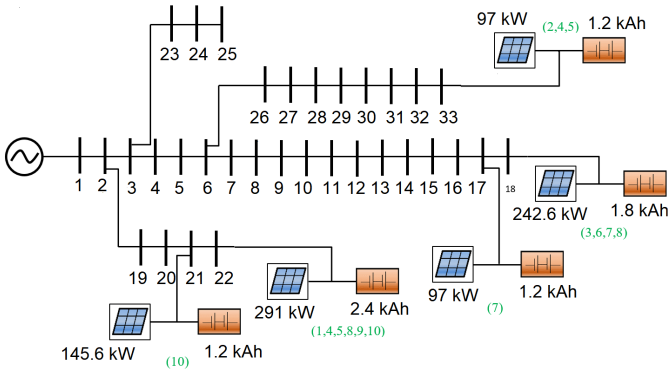

Fig. 3. The 33-bus distribution system with top 10 plans implemented for 100% coverage, showing rated solar array power and battery capacity along with options.

B. Lead-Acid Battery

Lead-acid batteries are combined with PV arrays for matching supply with demand. The battery can be charged during periods of surplus production and discharged when there is a deficit, so that the loads are always supplied. Grid-connected BESS can also be charged using grid supply. Allocation of batteries to each island is described by the following equations.

$$Q_{bs}^{(i)} \geq \frac{t_c \psi}{\eta_{bs\_inv}\eta_{ctrl}V_t MDOD} P^{US}(i) \tag{15}$$

Although commercial BESS are rated in electrical energy units (kWh or MWh), the ampere-hour capacity is more relevant to battery cells since the actual energy charge/discharge depends on the charging/discharging current. The ampere hour rating depends on the terminal voltage V_t. The maximum depth of discharge (MDOD), inverter efficiency η_{bs_inv} and charge controller efficiency η_{ctrl} are considered in the model described by (15). Since PV arrays provide no power during the night, a robust sizing strategy is used to decide the BESS capacity so that it can take on the entire unserved load by itself for a fixed duration of t_c hours, expected to be the maximum time required for service restoration. The BESS ampere-hour capacity $Q_{bs}^{(i)} = n_{bs}^{(i)} Q_{bs\_unit}$ installed in island i is made up of $n_{bs}^{(i)}$ battery cells, each with rated capacity of Q_{bs_unit}. Table II gives the details of the lead-acid battery cells used.

C. Annual Cost

The purpose of the planning model is the optimal sizing and allocation of the resources to enhance resilience and minimize total cost. This is formulated as an optimization problem with the total annual cost as the objective function and the various requirements, given by (13)–(15), enforced as constraints.

$$\min_{n_{pv}^{(i)}, n_{bs}^{(i)}} f_{cr}\left(C_{pv}\sum_i n_{pv}^{(i)} + C_{bs}\sum_i n_{bs}^{(i)}\right) + C_{pv\_OM}\sum_i P_{pv\_r}^{(i)} + C_{bs\_OM}\sum_i Q_{bs}^{(i)} \tag{16}$$

Total annualized cost is represented as expression in (16). The initial investment cost is found by multiplying the number of installed units by the cost per unit. C_{pv} and C_{bs} are the costs of each PV and BESS unit respectively, as specified in Tables I and II. The cost is annualized by multiplying it with the capital recovery factor $f_{cr} = r(1+r)^L/\{(1+r)^L - 1\}$, where r is the interest rate and L is the project lifetime. The annual operating and maintenance cost is calculated using the per unit capacity costs of PV and BESS, which are C_{pv_OM} and C_{bs_OM} respectively. Since resilience enhancement is the primary goal and normal operation is not a priority, fuel savings and tax credits are not included in the cost calculations, unlike in [36]. However, realistically a system planner would intend to use the PV generation and cheap electricity used to charge the BESS during off-peak hours to get added return on investment. These considerations would reduce the total annualized cost and provided a further incentive for generation expansion. It should be noted that due to the scope of this study, the test case does not include alternative grid hardening or redundancy-based measures, although these can also be incorporated into the proposed model as long as their costs and effects can be quantified.

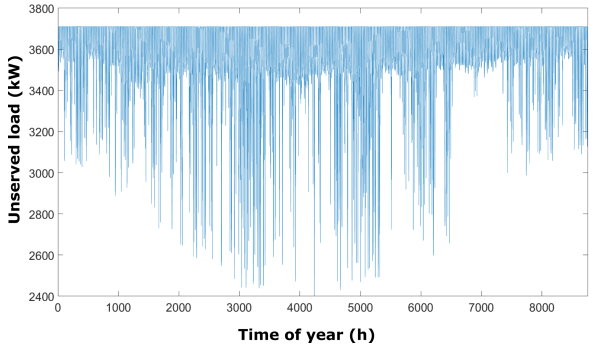

Fig. 4. Unserved load at different contingency occurrence time throughout the year, assuming battery backup is not available, based on hourly solar irradiance data.

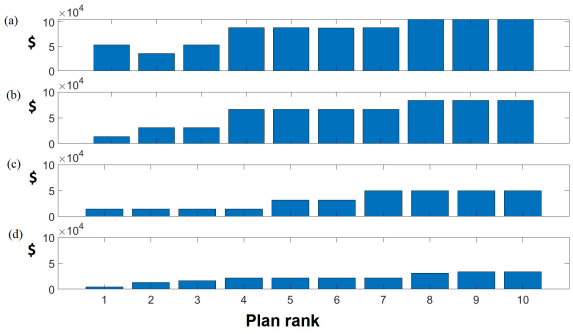

Fig. 5. Cost for the top 10 plans for (a) 100% (b) 99% (c) 95% and (d) 80% coverage.

IV. Case Study

Radial power distribution systems are particularly vulnerable to line outages, since disruption of a single line may cut off multiple buses from power. The proposed planning method is tested on the standard IEEE 33-bus system, a 12.66 kV radial

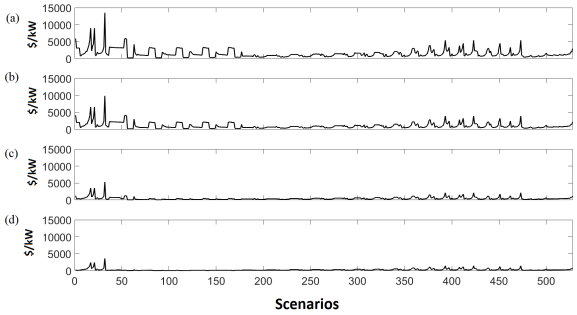

Fig. 6. Total cost-effectiveness for (a) 100% (b) 99% (c) 95% and (d) 80% coverage.

distribution system with total active and reactive power of 3.71 MW and 2.3 MVAR respectively [50]. Numerical solutions are obtained using CPLEX 12.8.0.0 optimization solver in MATLAB. All first- and second-order contingencies (one and two lines disabled, respectively) are simulated using the AC OPF model to yield the amount of unserved load at each node, considering all loads as dispatchable. The SOCP model is run for 528 contingencies. In the planning model, mixed-integer linear programming (MILP) is used to solve the optimization problem of minimizing total annual cost of additional PV and BESS systems for each contingency scenario. The numerical solution to the MILP problem gives the optimal plans for all scenarios, which are used as options in the AHP decision-making stage. Detailed parameters of PV panels and battery cells used in this study were obtained from [35].

A. Evaluation of Recommended Plans

The cost-effectiveness of each option for all scenarios is evaluated using (6). Plans are generally the least cost-effective for severe contingency scenarios (such as outage of the line between bus 1 and bus 2), where most of the buses are disconnected from the grid. These are the scenarios with the highest load shedding and require the most expensive plans. Comparison of the options on the basis of unserved load, cost, and utility (normalized with respect to the maximum), demonstrated in Fig. 2, show that costlier plans supply more power but generally tend to be less cost-effective. This trend of diminishing returns means that the planner must consider the trade-off between performance and cost-effectiveness using the decision support system described in Section II. Since the utility score is based on the pairwise comparison of plans, Fig. 2 indicates that cheaper plans are generally preferable to expensive ones. All options are ranked according to their AHP global scores based on the utility function in (4). The options are not mutually exclusive and often overlapping. For example, if Plan A requires a 728-cell array and Plan B requires a 1213-cell array at the same bus, then implementing Plan B makes Plan A redundant since it is effectively included in Plan B. The planner may choose to combine multiple options while staying within budget. Fig. 3 shows the result of implementing the first 10 plans recommended by AHP. The PV and BESS units are added preferentially to terminal buses, which are more vulnerable to load shedding due to being further away from the feeder.

B. Seasonal and Diurnal Variation

Diurnal and seasonal variations in solar irradiance results in variable power output from the PV arrays and means that the actual reduction in unserved load depends on the time of occurrence of the contingency. It is assumed that when the contingency occurs, the battery is at full capacity, charged by electricity from both the grid and PV arrays. Fig. 4 shows the amount of unserved load caused by the worst-case scenario, where the entire distribution network is disconnected from the source feeder, as the season and time of day of occurrence varies throughout the year. Hourly time-series data from the National Solar Radiation Database is used to estimate the variable power output of the PV arrays. Resilience enhancement is most effective during daytime around the middle of the year, when insolation is the highest. For this figure, Diffuse Horizontal Irradiance (DHI) data has been used to calculate the PV power output, assuming that the panels are fixed. The results can be significantly improved with the installation of sun-tracking systems for the panels, since Direct Normal Irradiance (DNI) is considerably higher than DHI.

TABLE III
PV CAPACITY (KW) BY LOCATION AND COVERAGE LEVEL

Cov (%)	Bus 8	Bus 14	Bus 17	Bus 18	Bus 21	Bus 22	Bus 25	Bus 32	Bus 33
100	0	0	97	242.6	145.6	291	0	0	97
80	0	78.4	0	8.6	0	27.6	0	71.4	0
60	10.6	74.6	0	0	0	0	80.8	101.8	0
40	6	3	0	1.2	0	0.8	0	9.8	0
20	0	78	0	38	0	0	91.8	444.8	0

TABLE IV
BESS CAPACITY (KAH) BY LOCATION AND COVERAGE LEVEL

Cov (%)	Bus 8	Bus 14	Bus 17	Bus 18	Bus 21	Bus 22	Bus 25	Bus 32	Bus 33
100	0	0	1.2	1.8	1.2	1.2	0	0	1.2
80	0	0.6	0	0.6	0	0.6	0	0.6	0
60	0.6	0.6	0	0	0	0	0.6	0.6	0
40	0.6	0.6	0	0.6	0	0.6	0	0.6	0
20	0	0.6	0	0.6	0	0	1.2	3.6	0

C. Coverage Level

The results shown in Figs. 2-3 have assumed that the planner intends to cover all of the unserved load with additional generation. The effect of reducing the total load coverage c, which may be necessary due to priorities and budget constraints, is also investigated in this case study. For some contingency scenarios where the unserved load is too low, the annualized cost of the optimal plan becomes zero and these scenarios are ignored in the AHP stage. Fig. 5 compares the cost of the top 10 plans for different levels of coverage. Fig. 6 does the same thing for total cost-effectiveness, defined as the sum of $CE_j^{(i)}$ for all contingencies i. The results show a significant reduction in total cost and cost per unit power as the coverage level is reduced from 100% to 80%. This fits the general trend of more expensive plans being more costly per kW. The average cost per kW of additional power capacity, calculated over all the plans and scenarios, is plotted for a broader range of coverage levels in Fig. 7. It shows that each unit of resilience enhancement becomes more expensive as larger proportions of loads are planned for. Assumed insolation is also a factor, since higher solar irradiance causes fewer panels to be installed for the same coverage level, resulting in lower investment cost and higher cost-effectiveness. Fig. 7 shows the cost-effectiveness for three insolation levels: the reference case, high insolation (+50%), and low insolation (–50%). Varying the coverage level

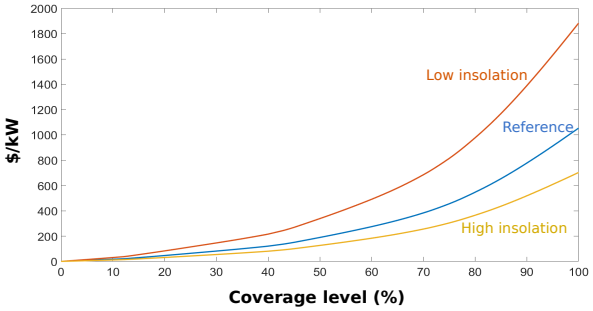

Fig. 7. Average cost-effectiveness for different levels of coverage and different amounts of insolation.

affects the location and capacity of resources added when the top 10 plans are implemented, as shown in Tables III and IV. Similar to Fig. 3, terminal bus locations tend to be favored. A reduction in target coverage does not necessarily reduce the installed capacity. As the coverage level is reduced, low-impact contingencies are increasingly removed from the pool and high-impact contingencies tend to be prioritized.

D. Planning Policy

Implementing the proposed framework requires the planner to make policy decisions. Fig. 1 shows that coverage level is a required input for the proposed method. Although 100% of the loads would be covered in an ideal situation, the planner may decide to lower the coverage level to below 100% to reduce costs. Therefore, coverage level is a matter of policy that must be set by the planner. Selecting plans would depend on the outcome of detailed cost-benefit analyses. One approach could be to use VoLL and expected energy not supplied (EENS) to determine if a particular set of plans is worth the investment. If C_a is the total annualized investment cost as given by (16) and the planner expects the distribution network to face a set of contingencies I over a year, then the following condition must be satisfied:

$$C_a < \sum_{i \in I} (EENS_0^{(i)} - EENS^{(i)}) * VoLL \qquad (17)$$

where $EENS^{(i)}$ and $EENS_0^{(i)}$ are the EENS values with and without the additional generation. The inequality essentially states that the reduction in annual monetary loss due to the extreme events must be greater than the annualized cost of the added resources. Final outcomes will depend on the VoLL used to find the monetary equivalent of lost load, as shown in Fig. 1. Calculation of per unit VoLL would be specific to the decision-maker's goals and is not considered in this study. Other benefits such as electricity bill savings and tax incentives can also be factored in to offset C_a. After ranking the plans in descending order of global scores, they are added to the distribution system one by one until the condition in (17) is violated. The largest set of plans obtained before the violation is then implemented.

V. Conclusion

This paper presents a flexible and generalizable decision-making framework that constitutes a systematic and quantitative approach to how additional investment can increase resilience and multiple alternative solutions can be ranked meaningfully. The proposed framework is intended to aid planners in decisions about the amount of resource allocation, on top of other hardening and redundancy-based measures that the planner intends to apply to the infrastructure. Contingency analysis by AC OPF is used as input for the planning stage, where PV and BESS resources are optimally allocated to supply loads. Since multiple contingencies are being considered and several plans are possible, AHP is used to choose between the available alternatives, ranked according to their cost-effectiveness across multiple scenarios. Lowering the coverage level is generally more cost-effective but may result in selection of expensive plans because the analysis is confined to high-impact contingencies that require large installed capacity. Therefore, planning policy suggestions are provided to help decision-makers evaluate the feasibility of solutions. The proposed method offers significant flexibility and transparency for decision-makers, as it allows insight into the range of options and how the cost-effectiveness scales with different decisions. Utility measures may be expanded beyond cost and resilience enhancement, as per the priorities of decision-makers. The utility function may be replaced by a different formula or an implicit system such as an expert system or learning algorithm. The set of scenarios may be expanded to include higher-order contingencies. Quantitative analysis reveals patterns can help planners compromise between cost and resilience, perhaps through a secondary decision support system. Since AHP only uses linear transformations and matrix operations, it may be scaled up to include more contingencies and allocation plans without requiring significantly greater computational power. The list of options in the case study of Section IV has been limited to the optimal plans for all scenarios, but the planning model may be expanded to generate any number of options, including other redundancy-based or grid hardening measures. However, simulation of numerous contingencies and allocation plans in large systems can be highly taxing. It may be necessary to limit the set of scenarios and plans to ensure computational tractability of numerical analyses preceding the AHP stage.

References

[1] J. H. Eto, K. H. LaCommare, M. D. Sohn, and H. C. Caswell, "Evaluating the Performance of the IEEE Standard 1366 Method for Identifying Major Event Days," *IEEE Trans. Power Syst.*, vol. 32, no. 2, pp. 1327–1333, Mar. 2017.

[2] Q. Chen and J. D. McCalley, "Identifying High Risk N-k Contingencies for Online Security Assessment," *IEEE Trans. Power Syst.*, vol. 20, no. 2, pp. 823–834, May 2005.

[3] P. Hines, J. Apt, and S. Talukdar, "Trends in the history of large blackouts in the United States," in *2008 IEEE Power and Energy Society General Meeting - Conversion and Delivery of Electrical Energy in the 21st Century*, 2008, pp. 1–8.

[4] Y. Wang, C. Chen, J. Wang, and R. Baldick, "Research on Resilience of Power Systems under Natural Disasters - A Review," *IEEE Trans. Power Syst.*, vol. 31, no. 2. pp. 1604–1613, Mar. 2016.

[5] E. S. Blake and D. A. Zelinsky, "Tropical Cyclone Report: Hurricane Harvey (AL092017)," Miami, FL, May 2018

[6] J. P. Cangialosi, A. S. Latto, and R. Berg, "Tropical Cyclone Report: Hurricane Irma (AL112017)," Miami, FL, Jun. 2018.

[7] K. Stouffer, V. Pillitteri, S. Lightman, M. Abrams, and A. Hahn, "Guide to Industrial Control Systems (ICS) Security," Nat. Inst. of Standards and Technology, SP 800-82 Rev. 2, Gaithersburg, MD, Jun. 2015.

[8] Y. Xiang, Z. Ding, Y. Zhang, and L. Wang, "Power System Reliability Evaluation Considering Load Redistribution Attacks," *IEEE Trans. Smart Grid*, vol. 8, no. 2, pp. 889–901, Mar. 2017.

[9] Y. Yuan, Z. Li, and K. Ren, "Quantitative Analysis of Load Redistribution Attacks in Power Systems," *IEEE Trans. Parallel Distrib. Syst.*, vol. 23, no. 9, pp. 1731–1738, Sep. 2012.

[10] O. Kosut, L. Jia, R. J. Thomas, and L. Tong, "Malicious data attacks on the smart grid," *IEEE Trans. Smart Grid*, vol. 2, no. 4, pp. 645–658, Dec. 2011.

[11] V. Venkataramanan, A. K. Srivastava, A. Hahn, and S. Zonouz, "Measuring and Enhancing Microgrid Resiliency against Cyber Threats," *IEEE Trans. Ind. Appl.*, vol. 55, no. 6, pp. 6303–6312, Nov. 2019.

[12] SANS Industrial Control Systems. (2016). *Analysis of the cyber attack on the Ukrainian power grid* [Online]. Available: https://ics.sans.org/media/E-ISAC_SANS_Ukraine_DUC_5.pdf

[13] N. N. Taleb, "On the statistical differences between binary forecasts and real-world payoffs," *Int. J. Forecast.*, Apr. 2020.

[14] The White House, "Presidential policy directive 21: Critical infrastructure security and resilience." pp. 37–53, 2014, Accessed: Jul. 18, 2018. [Online]. Available: https://obamawhitehouse.archives.gov/the-press-office/2013/02/12/presidential-policy-directive-critical-infrastructure-security-and-resil.

[15] Z. Bie, Y. Lin, G. Li, and F. Li, "Battling the Extreme: A Study on the Power System Resilience," *Proc. IEEE*, vol. 105, no. 7, pp. 1253–1266, Jul. 2017.

[16] T. R. B. Kushal and M. S. Illindala, "Correlation-based feature selection for resilience analysis of MVDC shipboard power system," *Int. J. Electr. Power Energy Syst.*, vol. 117, p. 105742, May 2020.

[17] M. Panteli and P. Mancarella, "The Grid: Stronger, Bigger, Smarter?: Presenting a Conceptual Framework of Power System Resilience," *IEEE Power Energy Mag.*, vol. 13, no. 3, pp. 58–66, May 2015.

[18] C. Chen, J. Wang, and D. Ton, "Modernizing Distribution System Restoration to Achieve Grid Resiliency Against Extreme Weather Events: An Integrated Solution," *Proc. IEEE*, vol. 105, no. 7, pp. 1267–1288, Jul. 2017.

[19] M. Panteli, C. Pickering, S. Wilkinson, R. Dawson, and P. Mancarella, "Power System Resilience to Extreme Weather: Fragility Modeling, Probabilistic Impact Assessment, and Adaptation Measures," *IEEE Trans. Power Syst.*, vol. 32, no. 5, pp. 3747–3757, Sep. 2017.

[20] G. Li et al., "Risk Analysis for Distribution Systems in the Northeast U.S. Under Wind Storms," *IEEE Trans. Power Syst.*, vol. 29, no. 2, pp. 889–898, Mar. 2014.

[21] S. Mukherjee, R. Nateghi, and M. Hastak, "A multi-hazard approach to assess severe weather-induced major power outage risks in the U.S.," *Reliab. Eng. Syst. Saf.*, vol. 175, pp. 283–305, Jul. 2018.

[22] L. Wu, M. Shahidehpour, and T. Li, "Stochastic security-constrained unit commitment," *IEEE Trans. Power Syst.*, vol. 22, no. 2, pp. 800–811, May 2007.

[23] A. Khodaei and M. Shahidehpour,"Microgrid-based co-optimization of generation and transmission planning in power systems," *IEEE Trans. Power Syst.*, vol. 28, no. 2, pp. 1582–1590, 2013.

[24] T. Amraee and H. Saberi, "Controlled islanding using transmission switching and load shedding for enhancing power grid resilience," *Int. J. Electr. Power Energy Syst.*, vol. 91, pp. 135–143, 2017.

[25] T. Ding, Y. Lin, Z. Bie, and C. Chen, "A resilient microgrid formation strategy for load restoration considering master-slave distributed generators and topology reconfiguration," *Appl. Energy*, vol. 199, pp. 205–216, 2017.

[26] H. Farzin, M. Fotuhi-Firuzabad, and M. Moeini-Aghtaie, "Enhancing Power System Resilience Through Hierarchical Outage Management in Multi-Microgrids," *IEEE Trans. Smart Grid*, vol. 7, no. 6, pp. 2869–2879, Nov. 2016.

[28] A. Dubey and S. Poudel, "A robust approach to restoring critical loads in a resilient power distribution system," in *IEEE Power and Energy Society General Meeting*, 2017, pp. 1–5.

[27] S. Chanda and A. K. Srivastava, "Defining and Enabling Resiliency of Electric Distribution Systems with Multiple Microgrids," *IEEE Trans. Smart Grid*, vol. 7, no. 6, pp. 2859–2868, Nov. 2016.

[29] Y. Fang and G. Sansavini, "Optimizing power system investments and resilience against attacks," *Reliab. Eng. Syst. Saf.*, vol. 159, pp. 161–173, Mar. 2017.

[30] S. Ma, B. Chen, and Z. Wang, "Resilience enhancement strategy for distribution systems under extreme weather events," *IEEE Trans. Smart Grid*, vol. 9, no. 2, pp. 1442–1451, Mar. 2018.

[31] R. Arghandeh et al., "The Local Team: Leveraging Distributed Resources to Improve Resilience," *IEEE Power Energy Mag.*, vol. 12, no. 5, pp. 76–83, Sep. 2014.

[32] W. D. Kellogg, M. H. Nehrir, G. Venkataramanan, and V. Gerez, "Generation unit sizing and cost analysis for stand-alone wind, photovoltaic, and hybrid wind/PV systems," *IEEE Trans. Energy Convers.*, vol. 13, no. 1, pp. 70–75, Mar. 1998.

[33] W. Kellogg, M. H. Nehrir, G. Venkataramanan, and V. Gerez, "Optimal unit sizing for a hybrid wind/photovoltaic generating system," *Electr. Power Syst. Res.*, vol. 39, no. 1, pp. 35–38, Oct. 1996.

[34] R. Chedid and S. Rahman, "Unit sizing and control of hybrid wind-solar power systems," *IEEE Trans. Energy Convers.*, vol. 12, no. 1, pp. 79–85, Mar. 1997.

[35] L. Xu, X. Ruan, C. Mao, B. Zhang, and Y. Luo, "An Improved Optimal Sizing Method for Wind-Solar-Battery Hybrid Power System," *IEEE Trans. Sustain. Energy*, vol. 4, no. 3, pp. 774–785, Jul. 2013.

[36] C. Yuan, M. S. Illindala, and A. S. Khalsa, "Co-Optimization Scheme for Distributed Energy Resource Planning in Community Microgrids," *IEEE Trans. Sustain. Energy*, vol. 8, no. 4, pp. 1351–1360, Oct. 2017.

[37] P. Denholm and R. M. Margolis, ''Evaluating the limits of solar photovoltaics (PV) in electric power systems utilizing energy storage and other enabling technologies," *Energy Policy*, vol. 35, no. 9, pp. 4424–4433, Sep. 2007.

[38] D. Álvaro, R. Arranz, and J. A. Aguado, "Sizing and operation of hybrid energy storage systems to perform ramp-rate control in PV power plants," *Int. J. Electr. Power Energy Syst.*, vol. 107, pp. 589–596, 2019.

[39] M. G. Kashani, M. Mobarrez, and S. Bhattacharya, "Smart Inverter Volt-Watt Control Design in High PV-Penetrated Distribution Systems," *IEEE Trans. Ind. Appl.*, vol. 55, no. 2, pp. 1147–1156, Mar. 2019.

[40] A. Ehsan and Q. Yang, "Optimal integration and planning of renewable distributed generation in the power distribution networks: A review of analytical techniques," *Appl. Energy*, vol. 210. Elsevier Ltd, pp. 44–59, Jan. 15, 2018.

[41] A. Ehsan and Q. Yang, "Coordinated Investment Planning of Distributed Multi-Type Stochastic Generation and Battery Storage in Active Distribution Networks," *IEEE Trans. Sustain. Energy*, vol. 10, no. 4, pp. 1813–1822, Oct. 2019.

[42] Y. Liu et al., "Bi-level planning model for optimal allocation of WT–PV–ESS in distribution networks," *J. Eng.*, vol. 2017, no. 13, pp. 1696–1701, Jan. 2017.

[43] R. Domínguez, A. J. Conejo, and M. Carrión, "Toward fully renewable electric energy systems," *IEEE Trans. Power Syst.*, vol. 30, no. 1, pp. 316–326, Jan. 2015.

[44] T. R. B. Kushal and M. S. Illindala, "A decision support framework for resilience-oriented cost-effective distributed generation expansion in power systems," in *IEEE/IAS 56th Ind. Commercial Power Syst. Tech. Conf.*, Las Vegas, NV, Jul. 2020, pp.1–8.

[45] A. Monticelli, M. V. F. Pereira, and S. Granville, "Security-Constrained Optimal Power Flow with Post-Contingency Corrective Rescheduling," *IEEE Trans. Power Syst.*, vol. 2, no. 1, pp. 175–180, 1987.

[46] X. Wu, A. J. Conejo, and N. Amjady, "Robust security constrained ACOPF via conic programming: Identifying the worst contingencies" *IEEE Trans. Power Syst.*, vol. 33, no. 6, pp. 5884–5891, Nov. 2018.

[47] R. A. Jabr, "Radial Distribution Load Flow Using Conic Programming," *IEEE Trans. Power Syst.*, vol. 21, no. 3, pp. 1458–1459, Aug. 2006.

[48] T. L. Saaty, "How to make a decision: The analytic hierarchy process," *Eur. J. Oper. Res.*, vol. 48, no. 1, pp. 9–26, Sept. 1990.

[49] Y. M. Atwa, E. F. El-Saadany, M. M. A. Salama, and R. Seethapathy, "Optimal renewable resources mix for distribution system energy loss minimization," *IEEE Trans. Power Syst.*, vol. 25, no. 1, pp. 360–370, 2010.

[50] M. E. Baran and F. F. Wu, "Network reconfiguration in distribution systems for loss reduction and load balancing," *IEEE Trans. Power Deliv.*, vol. 4, no. 2, pp. 1401–1407, Apr. 1989.